A CAD ENVIRONMENT FOR PERFORMANCE AND YIELD DRIVEN CIRCUIT DESIGN EMPLOYING ELECTROMAGNETIC FIELD SIMULATORS

J.W. Bandler, R.M. Biernacki, S.H. Chen
and P.A. Grobelny

OSA-93-OS-18-R

October 18, 1993

© Optimization Systems Associates Inc. 1993

A CAD ENVIRONMENT FOR PERFORMANCE AND YIELD DRIVEN CIRCUIT DESIGN EMPLOYING ELECTROMAGNETIC FIELD SIMULATORS

J.W. Bandler, R.M. Biernacki, S.H. Chen and P.A. Grobelny

Simulation Optimization Systems Research Laboratory
Department of Electrical and Computer Engineering
McMaster University, Hamilton, Canada L8S 4L7

Tel +1 905 525 9140 Ext. 24818
Fax +1 905 523 4407

E-mail: biernack@mcmail.cis.mcmaster.ca
or E-mail: bandler@mcmail.cis.mcmaster.ca

Technical Track: Computer-Aided Design

Preferred Presentation Format: Lecture

* J.W. Bandler, R.M. Biernacki and S.H. Chen are also with Optimization Systems Associates Inc., P.O. Box 8083, Dundas, Ontario, Canada L9H 5E7.

This work was supported in part by Optimization Systems Associates Inc. and in part by the Natural Sciences and Engineering Research Council of Canada under Grants OGP0042444, OGP0007239 and STR0117819.

A CAD ENVIRONMENT FOR PERFORMANCE AND YIELD DRIVEN CIRCUIT DESIGN EMPLOYING ELECTROMAGNETIC FIELD SIMULATORS

Abstract

In this paper we discuss a CAD environment for performance and yield driven circuit design with electromagnetic (EM) field simulations employed within the optimization loop. Microstrip structures are accurately simulated and their responses are incorporated into the overall circuit analysis. We unify the component level interpolation technique, devised to handle discretization of geometrical parameters, and the modeling technique used to lighten the computational burden of statistical design centering. We discuss the organization and utilization of our data base system integrated with the modeling technique. On several circuit design problems we demonstrate the feasibility and benefits of performance and yield optimization with EM simulations.

Extended Summary

INTRODUCTION

Electromagnetic (EM) simulators, though computationally intensive, are regarded as the most accurate at microwave frequencies. They also extend the validity of the models to higher frequencies, including millimeter-wave frequencies, and cover wider parameter ranges [1]. With the increasing availability of EM simulators [1-3] it is very tempting to include them into performance-driven and even yield-driven circuit optimization. Feasibility of such optimization has already been shown in our pioneering work [4,5].

In this paper we report new results on circuit design employing EM simulators directly driven by circuit level optimizers. We unify our interpolation technique, devised to reconcile continuously varying optimization variables with inherent discretization of geometrical parameters, and our modeling technique used for computationally intensive statistical design centering. In our work we utilize the OSA90/hope™ optimization environment [6] which allows us to select different optimizers, freely define responses and objectives, functionally interrelate variables, etc., and interact with external simulators. In particular, we use the Empipe [7] interface to the ***em***™ field simulator from Sonnet Software [3]. Applications include a double folded microstrip structure, one microstrip filter, a 3-section transformer and a small-signal amplifier.

EFFICIENT INTERPOLATION/MODELING

Numerical EM simulation is performed for discretized, or on-the-grid, values of geometrical parameters $\boldsymbol{x}$. Normally, gradient based optimizers handle continuously varying parameters. To facilitate it we interpolate the responses whenever the optimizer asks for simulation at an off-the-grid point. Our very efficient quadratic modeling technique [5,8-10] with linear modeling as a special case is extended and unified and to handle this geometrical interpolation.

The Q-model of a generic response $f(\boldsymbol{x})$ is a multidimensional quadratic polynomial of the form [8-10]

$$q(\boldsymbol{x}) = a_0 + \sum_{i=1}^{n} a_i(x_i - r_i) + \sum_{\substack{i=1 \\ j \geq i}}^{n} a_{ij}(x_i - r_i)(x_j - r_j) \tag{1}$$

where $\boldsymbol{x} = [x_1\ x_2\ \ldots\ x_n]^T$ is the vector of generic parameters in terms of which the response is defined, and $\boldsymbol{r} = [r_1\ r_2\ \ldots\ r_n]^T$ is a chosen reference point in the parameter space.

To build the Q-model we use $n + 1 \leq m \leq 2n + 1$ base points at which the function $f(\boldsymbol{x})$ is evaluated. The reference point $\boldsymbol{r}$ is selected as the first base point $\boldsymbol{x}^1$. The remaining $m - 1$ base points are selected by perturbing one variable at a time around $\boldsymbol{r}$ with a predetermined perturbation β_i. If a variable is perturbed twice the second perturbation is located symmetrically w.r.t. $\boldsymbol{r}$. By applying the Maximally Flat Quadratic Interpolation (MFQI) technique [8] to such a set of base points we obtain the following formula for the Q-model $q(\boldsymbol{x})$

$$q(\boldsymbol{x}) = f(\boldsymbol{r}) + \sum_{i=1}^{m-(n+1)} \left\{[f(\boldsymbol{x}^{i+1}) - f(\boldsymbol{x}^{n+1+i}) + (f(\boldsymbol{x}^{i+1}) + f(\boldsymbol{x}^{n+1+i}) - 2f(\boldsymbol{r}))(x_i - r_i)/\beta_i](x_i - r_i)/(2\beta_i)\right\}$$

$$+ \sum_{i=m-n}^{n} \left\{[f(\boldsymbol{x}^{i+1}) - f(\boldsymbol{r})](x_i - r_i)/\beta_i\right\} \tag{2}$$

Also, differentiating (2) w.r.t. x_i results in

$$\partial q(\boldsymbol{x})/\partial x_i = [(f(\boldsymbol{x}^{i+1}) - f(\boldsymbol{x}^{n+1+i}))/2 + (f(\boldsymbol{x}^{i+1}) + f(\boldsymbol{x}^{n+1+i}) - 2f(\boldsymbol{r}))(x_i - r_i)/\beta_i]/\beta_i \tag{3}$$

This formulation allows for a flexible choice of the number of base points starting at $m = n + 1$ which leads to the linear model, through linear/quadratic models w.r.t. selected variables, to the quadratic model w.r.t. all variables.

We consider two levels of discretization: physical and logical. The first one is imposed by the EM simulator. The grid size is specified for each of the parameters in the problem. Let the physical discretization matrix $\boldsymbol{\delta}_p$ be defined by the grid sizes Δx_i, Δy_i and Δz_i as

$$\boldsymbol{\delta}_p = \text{diag}\{\delta_{pi}\} = \text{diag}\{\Delta x_1, \Delta x_2, \ldots, \Delta y_1, \Delta y_2, \ldots, \Delta z_1, \Delta z_2, \ldots\} \tag{4}$$

A specific EM simulator may allow only one grid size for each orientation while others may provide the flexibility of independent Δx_i, Δy_i and Δz_i for different parameters of the same x, y, or z orientation. For uniform discretization in each direction $\Delta x_i = \Delta x$, $\Delta y_i = \Delta y$ and $\Delta z_i = \Delta z$.

The logical discretization is superimposed on top of the physical grid. Let the logical discretization matrix $\boldsymbol{\delta}_l$ be defined as

$$\boldsymbol{\delta}_l = \text{diag}\{\delta_{li}\} = \text{diag}\{\delta_{lx1}, \delta_{lx2}, ..., \delta_{ly1}, \delta_{ly2}, ..., \delta_{lz1}, \delta_{lz2}, ...\} \tag{5}$$

The physical grid sizes are floating point numbers and have the same units as the corresponding parameters. The logical grid sizes are unitless integers. The distance between adjacent logical grid points is an integer multiple (δ_{li} for the ith parameter) of the physical grid size. The first logical grid point is aligned with the first nonzero physical grid point. The subset of physical grid points for a parameter determined by the logical grid points are called the permitted grid points. Fig. 1 illustrates the relation between the physical and logical grid points.

To utilize the Q-modeling technique for geometrical interpolation we first generate a set of m base points called the interpolation base $\boldsymbol{B}$. The reference point $\boldsymbol{r}$ is selected as the first base point $\boldsymbol{x}^1$ by snapping $\boldsymbol{x} = [x_1\ x_2\ ...\ x_n]^T$ to the closest (in the ℓ_2 sense) permitted grid point. Matrix $\boldsymbol{\theta}$ defines the relative deviation of $\boldsymbol{x}$ from $\boldsymbol{r}$ and is obtained from

$$\boldsymbol{\theta} = \text{diag}\{\theta_i\} = \text{diag}\{\theta_1, \theta_2, ..., \theta_n\} \tag{6}$$

where

$$\theta_i = (x_i - r_i)/(\delta_{pi}\delta_{li}), \quad i = 1, 2, ..., n \tag{7}$$

The other base points are created by perturbing one variable at a time around $\boldsymbol{r}$. The magnitude of the perturbation β_i is $\delta_{pi}\delta_{li}$. These base points can then be expressed as

$$\boldsymbol{x}^{i+1} = \boldsymbol{r} + [0\ ...\ 0\ \ +\delta_{pi}\delta_{li}\ \ 0\ ...\ 0]^T, \quad i = 1, ..., n \tag{8a}$$

$$\boldsymbol{x}^{n+1+i} = \boldsymbol{r} + [0\ ...\ 0\ \ -\delta_{pi}\delta_{li}\ \ 0\ ...\ 0]^T, \quad m - (n + 1) \tag{8b}$$

For each Q-model we define a validity region V. If $x \in V$ than we assume that the model is valid and that $q(x) \approx f(x)$. If $x \notin V$ the model $q(x)$ must be updated. One possible choice for V is given by

$$V = \{x \mid (x_i - r_i) \leq \beta_i/2, (r_i - x_i) < \beta_i/2\}, \quad i = 1, 2, ..., n \tag{9}$$

Fig. 2 graphically depicts the selection of base points for a two-dimensional example together with the corresponding model validity region V.

It is evident from (2) that if a certain x_i coincides with a permitted grid coordinate then the contribution of x_i to $q(x)$ is zero. Therefore, the base point x^{i+1} need not be simulated and does not have to be included in the interpolation base B.

MULTILEVEL MODELING

Multilevel modeling is depicted schematically in Fig. 3. The circuit under consideration is divided into subcircuits, possibly in a hierarchical manner. At the lowest level we have circuit components, e.g., a lumped capacitor or a microstrip structure.

Defining f_c, f_s and f_e as circuit, subcircuit and component responses, respectively, we can express the response of the circuit as a function of the subcircuit responses which are in turn functions of component responses. This hierarchy can be expressed formally as

$$f_c = f_c(f_{s1}, f_{s2}, ..., f_{sn_s}) \tag{10}$$

$$f_{si} = f_{si}(f_{ei1}, f_{ei2}, ..., f_{ein_{ei}}), \quad i = 1, 2, ..., n_s \tag{11}$$

and

$$f_{eij} = f_{eij}(x), \quad i = 1, 2, ..., n_s, \quad j = 1, 2, ..., n_{ei} \tag{12}$$

where n_s is the number of subcircuits and n_{ei} is the number of components in the ith subcircuit. x is the vector of circuit parameters. The responses are typically frequency-domain functions of multiport responses.

We can create a single Q-model for the overall circuit. We can also create a hierarchy of Q-models to represent some or all of the subcircuits and components, as illustrated in Fig. 3. By applying Q-modeling technique to geometrical interpolation outlined in the preceding section we effectively unify the overall multilevel modeling approach and address it in a consistent manner at all levels of hierarchy. This includes extending the concept of the interpolation base to higher levels of hierarchy.

INTEGRATED DATA BASE/MODELING SUBSYSTEM

Let the set of base points for a Q-model be defined by $[\boldsymbol{x}^1 \; \boldsymbol{x}^2 \; \ldots \; \boldsymbol{x}^m]^T$, where $\boldsymbol{x}^1$ is the reference point $\boldsymbol{r}$, $n + 1 \leq m \leq 2n + 1$, and n is the number of model parameters. Then we can express the simulation results at these base points as

$$[\boldsymbol{f}(\boldsymbol{x}^1) \; \boldsymbol{f}(\boldsymbol{x}^2) \; \ldots \; \boldsymbol{f}(\boldsymbol{x}^m)] \tag{13}$$

with

$$\boldsymbol{f}(\boldsymbol{x}^i) = [f_1(\boldsymbol{x}^i) \; f_2(\boldsymbol{x}^i) \; \ldots \; f_k(\boldsymbol{x}^i)]^T, \quad i = 1, 2, \ldots, m \tag{14}$$

where k is the total number of different responses. $\boldsymbol{f}$ can be a response of the overall circuit, a subcircuit or a component. Then

$$\boldsymbol{f}(\boldsymbol{x}) \approx \boldsymbol{q}(\boldsymbol{x}) = [q_1(\boldsymbol{x}) \; q_2(\boldsymbol{x}) \; \ldots \; q_k(\boldsymbol{x})]^T \tag{15}$$

The Q-models in (15) approximate $\boldsymbol{f}(\boldsymbol{x})$ for $\boldsymbol{x}$ belonging to the Q-model validity region $\boldsymbol{V}$ centered around the reference point $\boldsymbol{r} = \boldsymbol{x}^1$.

The nominal point moves during optimization, and so does, in the case of yield optimization, the set of associated statistical outcomes. This may result in parameter values of the nominal point as well as of some or even all the statistical outcomes to be outside of the validity region $\boldsymbol{V}$ of the current Q-models. We have developed a scheme in which the Q-models are automatically updated in real optimization time. If a point at which simulation is requested by the optimizer falls outside the current $\boldsymbol{V}$, a new set of base points is generated, the responses at these base points are simulated *but only if they have not been simulated previously*, and updated Q-models are generated.

In order to properly utilize the results (13), in particular of expensive EM simulations, and to avoid repeated simulations, we maintain a data base $\boldsymbol{D}$ of the already simulated base points together with the corresponding responses. These results are stored and accessed when necessary (see Fig. 4). Each time simulation is requested the corresponding interpolation base $\boldsymbol{B}$ is generated and checked against the existing data base. Actual simulation is invoked only for the base points not present in the data base ($\boldsymbol{B}$ - $\boldsymbol{D}$). Results for the base points already present in the data base ($\boldsymbol{B} \cap \boldsymbol{D}$) are simply retrieved from $\boldsymbol{D}$ and used for interpolation. The data base and the Q-models are automatically updated whenever new simulation results become available.

APPLICATIONS

Our new unified multilevel modeling technique has been tested using ***em*** [3] from Sonnet Software, Inc., interfaced to OSA90/hope [6] from Optimization Systems Associates Inc., through Empipe [7], accordingly modified. We have performed thorough investigation of several benchmark circuit design problems including performance-driven optimization, statistical Monte Carlo analysis, yield optimization, as well as yield sensitivity analysis. In the final version of the paper we will report the results on the following circuits.

A Double Folded Microstrip Structure for band-stop filter applications, shown in Fig. 5. This structure may substantially reduce the filter area while achieving the same goal as the conventional double stub structure [11]. The symmetrical double folded stub can be described by 4 parameters: width, spacing and two lengths W, S, L_1 and L_2, as marked in Fig. 5.

A 26-40 GHz Interdigital Microstrip Filter, shown in Fig. 6. This millimeter-wave bandpass filter was designed and built on a 10 mils thick substrate with relative dielectric constant of 2.25. There is a total of 13 designable parameters including the distance between the patches L_1, the finger length L_2 and two patch widths W_1 and W_2 for each of the three interdigital capacitors, and the length L of the end capacitor.

A 3-section Microstrip Transformer, shown in Fig. 7. The source and load impedances are 50 and 150 ohms, respectively. The design specification is set for input reflection coefficient as

$$|S_{11}| \leq 0.12, \text{ from 5 GHz to 15 GHz}$$

The error functions for yield optimization are calculated for frequencies from 5 GHz to 15 GHz with a 0.5 GHz step. The transformer is built on a 0.635 mm thick substrate with relative dielectric constant 9.7.

A Singe-Stage 6-18 GHz Small-Signal Amplifier, shown in Fig. 8, with the specification

$$7 \text{ dB} \leq |S_{21}| \leq 8 \text{ dB, from 6 GHz to 18 GHz}$$

The microstrip components of the amplifier are simulated by ***em*** while analysis and optimization of the overall circuit is performed by OSA90/hope. The gate and drain circuit microstrip T-junctions and the feedback microstrip line are built on a 10 mil thick substrate with relative dielectric constant 9.9.

CONCLUSIONS

We have discussed a CAD environment for performance and yield driven design of circuits employing accurate EM field simulations. It includes an efficient modeling technique used to decrease the computational burden and overcome problems related to the discrete nature of EM simulation. We have outlined the organization and utilization of our data base system integrated with the modeling technique. We have investigated several circuit design problems which clearly demonstrate the feasibility and benefits of both performance and yield optimization with EM simulations invoked within the optimization loop. Full description of these applications will be included in the final version of this paper.

REFERENCES

[1] T. Itoh, Ed., *Numerical Techniques for Microwave and Millimeter-Wave Passive Structures.* New York: Wiley, 1989.

[2] R.H. Jansen and P. Pogatzki, "A hierarchically structured, comprehensive CAD system for field theory-based linear and nonlinear MIC/MMIC design," *1992 2nd Int. Workshop of the German IEEE MTT/AP Joint Chapter on Integrated Nonlinear Microwave and Millimeterwave Circuits Dig.* (Duisburg, Germany), 1992, pp. 333-341.

[3] *Em User's Manual* and *Xgeom User's Manual*, Sonnet Software, Inc., 135 Old Cove Road, Suite 203, Liverpool, NY 13090-3774, May 1992.

[4] J.W. Bandler, S. Ye, R.M. Biernacki, S.H. Chen and D.G. Swanson, Jr., "Minimax microstrip filter design using direct EM field simulation," *IEEE MTT-S Int. Microwave Symp. Dig.* (Atlanta, GA), 1993, pp. 889-892.

[5] J.W. Bandler, R.M. Biernacki, S.H. Chen, P.A. Grobelny and S. Ye, "Yield-driven electromagnetic optimization via multilevel multidimensional models," *IEEE Trans. Microwave Theory Tech.*, vol. 41, December, 1993.

[6] *OSA90/hope™ Version 2.5 User's Manual*, Optimization Systems Associates Inc., P.O. Box 8083, Dundas, Ontario, Canada L9H 5E7, 1993.

[7] *Empipe™ Version 1.1 Technical Brief*, Optimization Systems Associates Inc., P.O. Box 8083, Dundas, Ontario, Canada L9H 5E7, 1993.

[8] R.M. Biernacki and M.A. Styblinski, "Efficient performance function interpolation scheme and its application to statistical circuit design," *IEEE Int. J. Circuit Theory and Appl.*, vol. 19, 1991, pp. 403-422.

[9] R.M. Biernacki, J.W. Bandler, J. Song and Q.J. Zhang, "Efficient quadratic approximation for statistical design," *IEEE Trans. Circuits and Systems*, vol. 36, 1989, pp. 1449-1454.

[10] J.W. Bandler, R.M. Biernacki, S.H. Chen, J. Song, S. Ye and Q.J. Zhang, "Gradient quadratic approximation scheme for yield-driven design," *IEEE MTT-S Int. Microwave Symp. Dig.* (Boston, MA), 1991, pp. 1197-1200.

[11] J.C. Rautio, Sonnet Software, Inc., 135 Old Cove Road, Suite 203, Liverpool, NY 13090-3774, Private communication, 1992.

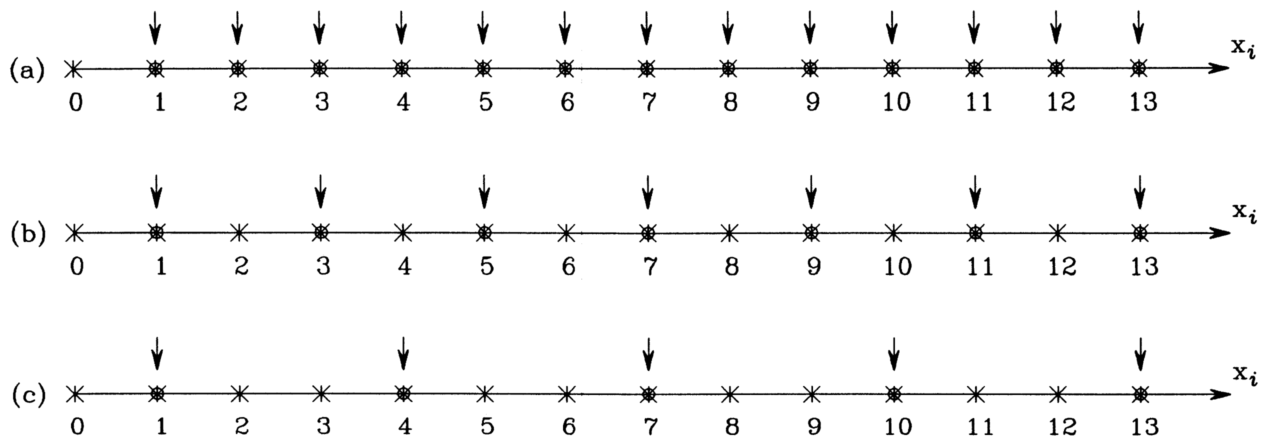

Fig. 1 The relation between the physical (×) and logical (○) grids. The physical grid is set to 1.0. The logical grid is set to 1 (a), 2 (b) and 3 (c). The permitted grid points are indicated by arrows. Simulation can be performed only at the permitted grid points.

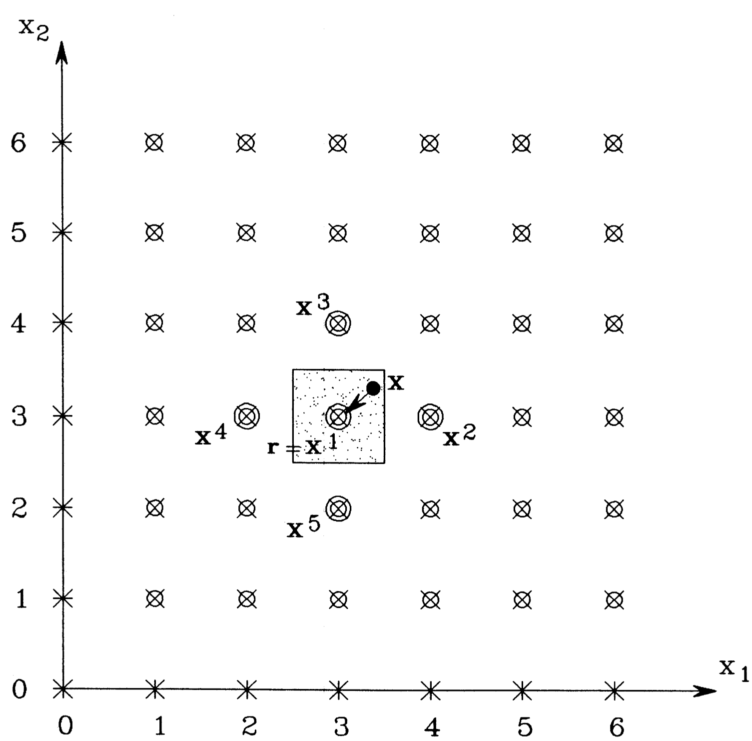

Fig. 2 Selection of base points in two dimensions for the Q-model and $\delta_p = \delta_l = 1$. x is snapped to r ($r = x^1$). x^2, x^3, x^4 and x^5 are the other base points. Interpolation base $B = \{x^1\ x^2\ x^3\ x^4\ x^5\}$. The shaded area around r indicates the model validity region V. ⊗ indicate the permitted base points.

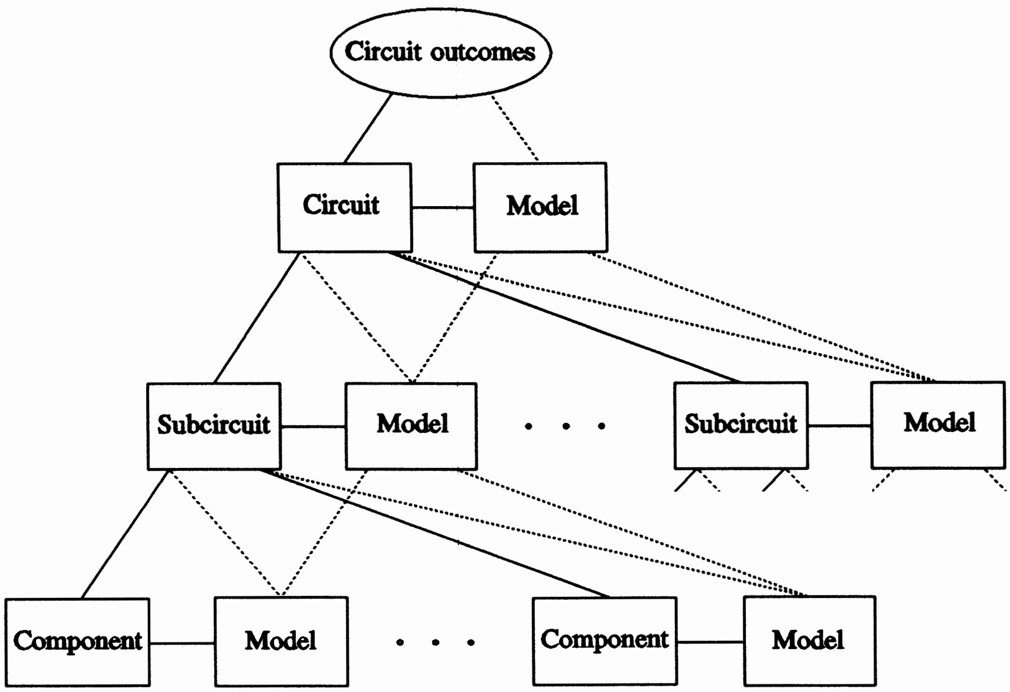

Fig. 3 Schematic diagram illustrating multilevel modeling. Solid and dotted lines distinguish simulated and modeled responses.

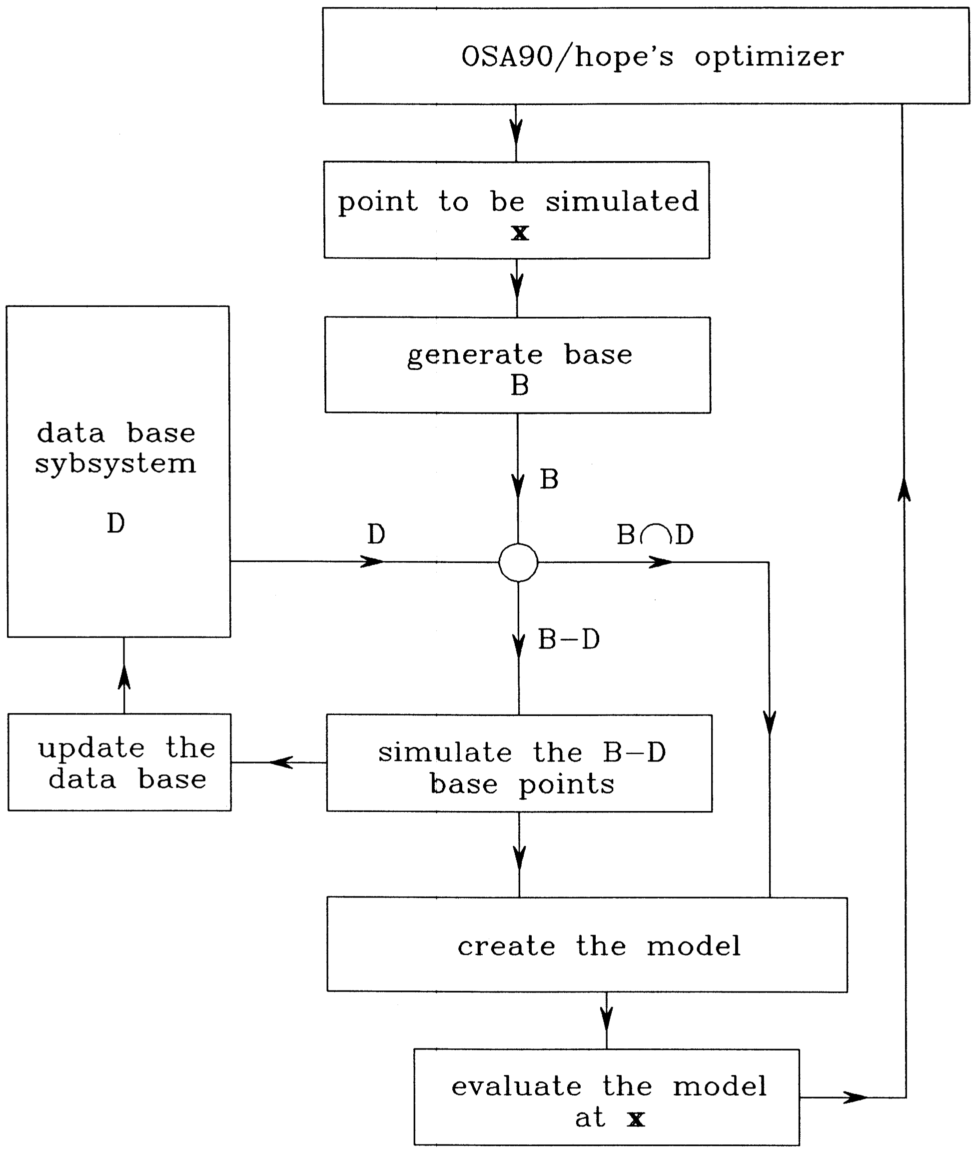

Fig. 4 **Flow diagram illustrating the interconnection between an OSA90/hope optimizer and an external (EM) simulator.**

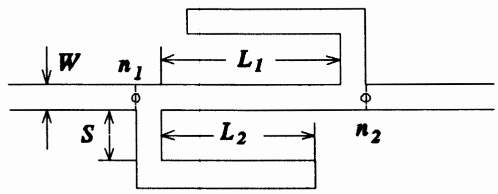

Fig. 5 Double folded stub microstrip structure for band-stop filter applications.

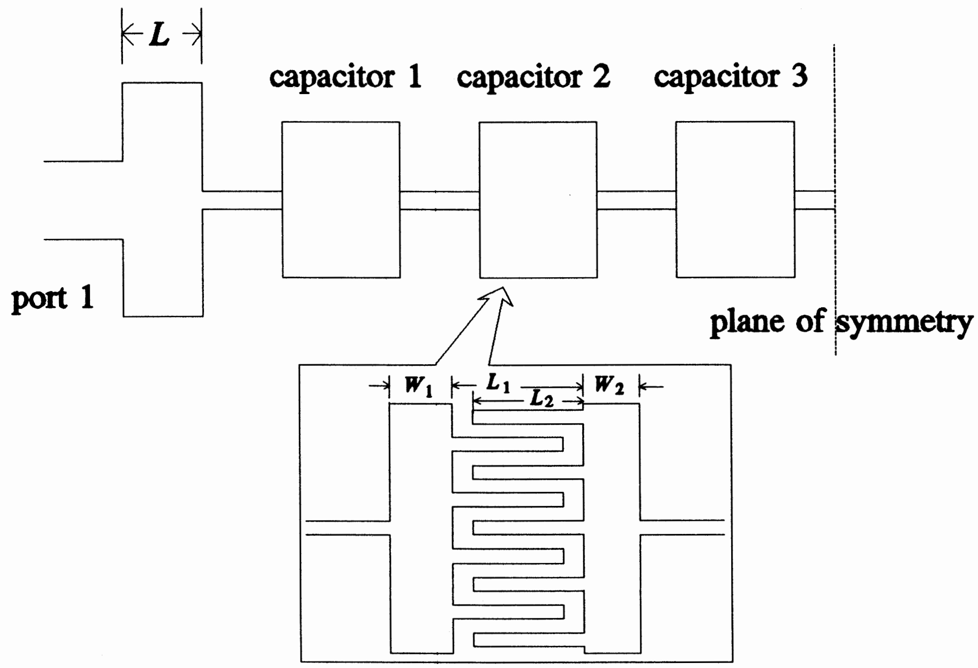

Fig. 6 The 26-40 GHz interdigital capacitor filter. The dielectric constant is 2.25. Substrate thickness and shielding height are 10 and 120 mils, respectively. The optimization variables include L, and L_1, L_2, W_1, W_2 for each capacitor, totalling 13.

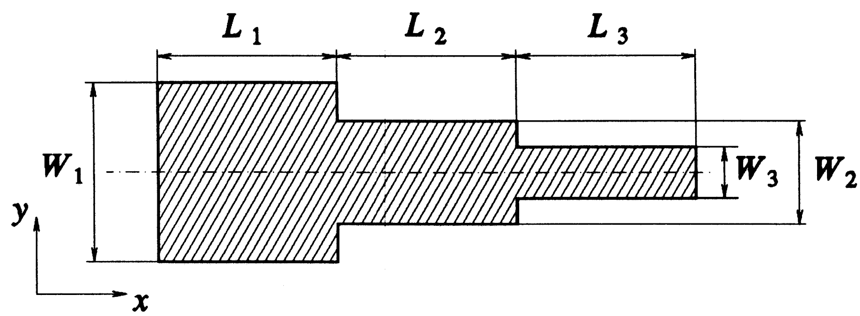

Fig. 7 The 3-section 3:1 microstrip impedance transformer. The thickness and dielectric constant of the substrate are 0.635 mm and 9.7, respectively.

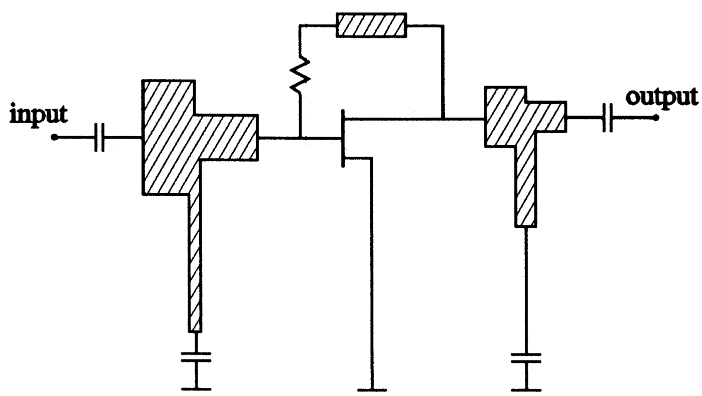

Fig. 8 Circuit diagram of the 6-18 GHz small-signal amplifier. We use ***em*** to model the two T-junction structures and the microstrip line.